Molecular and Cellular Neuroscience 52 (2013) 161–172

Contents lists available at SciVerse ScienceDirect

Molecular and Cellular Neuroscience

journal homepage: www.elsevier.com/locate/ymcne

Differential regulation of evoked and spontaneous neurotransmitter release by C-terminal modifications of complexin

Lauren K. Buhl, Ramon A. Jorquera [1], Yulia Akbergenova, Sarah Huntwork-Rodriguez, Dina Volfson, J. Troy Littleton *

Department of Brain and Cognitive Sciences, Department of Biology, The Picower Institute for Learning and Memory, Massachusetts Institute of Technology, Cambridge, MA 02139, United States

ARTICLE INFO

Article history:
Received 30 May 2012
Revised 10 September 2012
Accepted 7 November 2012
Available online 16 November 2012

Keywords:
Exocytosis
Synapse
Neurotransmitter release
Synaptic vesicle
SNARE complex

ABSTRACT

Complexins are small α-helical proteins that modulate neurotransmitter release by binding to SNARE complexes during synaptic vesicle exocytosis. They have been found to function as fusion clamps to inhibit spontaneous synaptic vesicle fusion in the absence of Ca^{2+}, while also promoting evoked neurotransmitter release following an action potential. Complexins consist of an N-terminal domain and an accessory α-helix that regulates the activating and inhibitory properties of the protein, respectively, and a central α-helix that binds the SNARE complex and is essential for both functions. In addition, complexins contain a largely unstructured C-terminal domain whose role in synaptic vesicle cycling is poorly defined. Here, we demonstrate that the C-terminus of *Drosophila* complexin (DmCpx) regulates localization to synapses and that alternative splicing of the C-terminus can differentially regulate spontaneous and evoked neurotransmitter release. Characterization of the single *DmCpx* gene by mRNA analysis revealed expression of two alternatively expressed isoforms, DmCpx7A and DmCpx7B, which encode proteins with different C-termini that contain or lack a membrane tethering prenylation domain. The predominant isoform, DmCpx7A, is further modified by RNA editing within this C-terminal region. Functional analysis of the splice isoforms showed that both are similarly localized to synaptic boutons at larval neuromuscular junctions, but have differential effects on the regulation of evoked and spontaneous fusion. These data indicate that the C-terminus of *Drosophila* complexin regulates both spontaneous and evoked release through separate mechanisms and that alternative splicing generates isoforms with distinct effects on the two major modes of synaptic vesicle fusion at synapses.

Introduction

A conserved vesicle trafficking machinery made up of soluble N-ethylmaleimide-sensitive factor attachment protein receptors (SNAREs) and SM proteins drives membrane fusion in multiple cellular compartments (Südhof and Rothman, 2009). At synapses, the fusion of neurotransmitter containing vesicles with the plasma membrane is tightly regulated to allow for precise communication within the nervous system. Several SNARE-binding accessory proteins that modulate the activity of the core machinery have evolved to provide synapse-specific requirements for synaptic vesicle fusion. The best studied of these accessory proteins is the vesicular Ca^{2+} sensor synaptotagmin 1 (Syt 1), which binds to SNARE complexes and membrane phospholipids in a Ca^{2+}-dependent manner to allow for fast synchronous neurotransmitter release in response to Ca^{2+} (Geppert et al., 1994; Xu et al., 2007; Yoshihara and Littleton, 2002). In contrast to Syt 1, the precise function of complexin (Cpx) in synaptic vesicle fusion is still being elucidated. Cpxs are small, α-helical proteins identified based on their ability to bind the assembled SNARE complex with 1:1 stoichiometry (Bracher et al., 2002; Chen et al., 2002; McMahon et al., 1995; Pabst et al., 2000).

Numerous studies have suggested that Cpx acts both to inhibit spontaneous neurotransmitter release in the absence of Ca^{2+} (Hobson et al., 2011; Huntwork and Littleton, 2007; Martin et al., 2011; Maximov et al., 2009) and to promote evoked neurotransmitter release (Cai et al., 2008; Hobson et al., 2011; Huntwork and Littleton, 2007; Martin et al., 2011; Maximov et al., 2009; Reim et al., 2001; Xue et al., 2007, 2008). Data from biochemical studies (Giraudo et al., 2006; Schaub et al., 2006), genetic knock-out studies in *Drosophila* and *Caenorhabditis elegans* (Hobson et al., 2011; Huntwork and Littleton,

Abbreviations: NMJ, neuromuscular junction; EJP, excitatory junctional potential; Cpx, complexin; m, mouse; SNARE, soluble N-ethylmaleimide-sensitive fusion attachment protein receptor; Dm, *Drosophila melanogaster*; SEM, standard error of the mean; HRP, horse radish peroxidase; UTR, untranslated region.

* Corresponding author at: Massachusetts Institute of Technology, 43 Vassar Street, 46-3243, Cambridge, MA 02139, United States. Fax: +1 617 452 2249.
E-mail address: troy@mit.edu (J.T. Littleton).
[1] Present Address: Neuroscience Department, Universidad Central del Caribe, Bayamon, Puerto Rico.

1044-7431/$ – see front matter © 2012 Elsevier Inc. All rights reserved.
http://dx.doi.org/10.1016/j.mcn.2012.11.009

2007; Martin et al., 2011) and genetic knock-down studies in mice (Maximov et al., 2009) have supported the role of Cpx as an inhibitor of spontaneous neurotransmitter release. Genetic deletion of the single Cpx homolog in *Drosophila* (DmCpx) results in a dramatic increase in the frequency of spontaneous vesicle fusion events (minis) at the larval neuromuscular junction (NMJ) (Cho et al., 2010; Huntwork and Littleton, 2007). Similarly, the frequency of tonic fusion events at the *C. elegans* NMJ is increased in genetic knock-outs of the primary Cpx homolog (CeCpx-1) (Hobson et al., 2011; Martin et al., 2011). Unlike flies and worms, mammals have four Cpx genes with distinct expression patterns in the nervous system (Reim et al., 2005). RNAi knock-down of Cpxs in mouse cortical cultures increases spontaneous neurotransmitter release (Maximov et al., 2009). However, genetic knock-out of Cpxs results in decreased spontaneous neurotransmitter release at hippocampal autapses and GABA-/glycinergic synapses, but not at striatal autapses (Strenzke et al., 2009; Xue et al., 2007, 2008).

In contrast to the different findings on spontaneous fusion, studies have consistently shown that Cpx is necessary to promote evoked Ca^{2+}-dependent neurotransmitter release. These data indicate that Cpx has distinct effects on different modes of neurotransmitter release and plays several roles during the multi-step process of synaptic vesicle fusion. Structure–function studies suggest that different domains of Cpx contribute to specific steps in synaptic vesicle trafficking. A central helix within Cpx is necessary for SNARE binding as determined by crystallography (Bracher et al., 2002; Chen et al., 2002). Cpx constructs that lack this domain or key binding residues within it are non-functional (Cho et al., 2010; Giraudo et al., 2008; Martin et al., 2011; Maximov et al., 2009; Xue et al., 2007). The N-terminus, meanwhile, appears to contain both facilitatory and inhibitory domains that may be differently used at mammalian and invertebrate synapses (Giraudo et al., 2009; Hobson et al., 2011; Martin et al., 2011; Xue et al., 2007, 2009, 2010). In contrast, the function of the C-terminus is poorly understood. Biochemical studies have shown that the C-terminus inhibits SNARE-mediated cell fusion but promotes cell-mediated liposome fusion (Giraudo et al., 2008; Malsam et al., 2009). In addition, Cpx constructs that lack the C-terminus are functional in hippocampal autapses, yet fail to rescue the increased tonic neurotransmitter release observed at the *C. elegans* NMJ in *cpx-1* null mutants, suggesting that the C-terminus may act to inhibit neurotransmitter release at some synapses. Recent studies of several mammalian Cpx isoforms suggest the C-terminal domain may differentially regulate clamping versus activation properties of different isoforms (Kaeser-Woo et al., 2012). Given these divergent results, additional characterization of the C-terminus is needed to define its precise role in synaptic transmission.

In this study, we analyzed the function of the C-terminus of DmCpx. Using a chemical mutagenesis approach, we isolated a *Cpx* allele with an early stop codon that truncates the far C-terminus. These mutants show reduced Cpx protein levels and mislocalize Cpx at synaptic boutons at *Drosophila* larval NMJs. We subsequently identified two alternatively spliced isoforms, DmCpx7A and DmCpx7B, which vary in the far C-terminus, with additional C-terminal variation created through RNA editing of DmCpx7A. Although DmCpx7A predominates at the mRNA level in larvae and adults, both isoforms are expressed in the developing nervous system and their mRNA expression is activity-regulated. In transgenic rescue experiments, we show that DmCpx7A and DmCpx7B are similarly localized to synaptic boutons at the larval NMJ. However, we find that DmCpx7A and DmCpx7B have different effects on spontaneous and evoked neurotransmitter release, with DmCpx7A being a better inhibitor of spontaneous release and DmCpx7B functioning as a better facilitator of evoked release. DmCpx7A contains a C-terminal membrane tethering prenylation domain, while DmCpx7B does not. We propose a model in which C-terminal modification regulates the effects of Cpx on different modes of neurotransmitter release.

Results

The C-terminus of DmCpx is necessary for protein stability, localization and function

We performed an ethane methylsulfonate (EMS) non-complementation mutagenesis screen with the cpx^{SH1} null mutant to isolate additional *Cpx* alleles in *Drosophila*. cpx^{572} was identified in a screen of 5000 mutagenized lines as a loss-of-function mutation. Sequence analysis revealed that the cpx^{572} allele contains a small deletion near the end of exon 6, leading to a premature stop codon and deletion of the final ~25 residues of the Cpx protein (Fig. 1A). Similar to the cpx^{SH1} null allele (Huntwork and Littleton, 2007), cpx^{572} is semi-lethal. Homozygous adult cpx^{572} escapers are uncoordinated and ataxic, though they are less severely affected than null animals. Western blot analysis indicates that a truncated form of Cpx protein is present in head extracts from cpx^{572} adults. The truncated Cpx protein is expressed at <20% of wild type levels (Fig. 1B), suggesting that the far C-terminus regulates Cpx protein stability in vivo.

We next evaluated Cpx protein localization and function at larval NMJs of cpx^{572} mutants. Although weak Cpx expression could be detected within motor axons, Cpx failed to accumulate in synaptic boutons at similar levels to the wildtype protein when examined by confocal microscopy (Fig. 1C). Imaging at higher laser power revealed that the remaining Cpx found at mutant cpx^{572} NMJs was distributed in puncta, rather than being localized diffusely in the bouton as observed in controls (Fig. 1D). The Cpx puncta found at cpx^{572} NMJs resided near, but did not completely overlap active zones, as revealed by co-staining for the active zone protein Bruchpilot. The residual Cpx did not overlap with peri-active zone proteins such as Fas2 (Fig. 1D). These data indicate that the far C-terminus of Cpx regulates its subsynaptic localization. In addition to mislocalization of Cpx at synapses, cpx^{572} larvae displayed disruptions in synaptic transmission at the NMJ, with a slightly less severe phenotype than observed in cpx^{SH1} null larvae (Fig. 2). cpx^{572} mutants show a large elevation in the frequency of spontaneous release (Fig. 2A, B), and a milder reduction in the amplitude of the evoked response compared to nulls (Fig. 2C, D). Compared to cpx^{SH1} null mutants, cpx^{572} mutants also showed milder defects in synaptic depression during short (Fig. 2E, F) and long (Fig. 2G–I) stimulation trains. These data indicate that the C-terminus regulates both subsynaptic localization and function of Cpx, and that the cpx^{572} mutant is a hypomorphic allele.

The Drosophila Cpx locus generates multiple splice isoforms

To further investigate the function of the C-terminus of DmCpx, we used cDNA analysis to detect any endogenous sequence variation present at the *Cpx* genomic locus. Unlike mammals, which have four Cpx genes, there is only a single *Cpx* gene in *Drosophila*. An analysis of the genomic sequence compared to sequenced expressed sequence tag (EST) clones revealed multiple alternative splicing predictions for *DmCpx* (Fig. 3A). The genomic locus is predicted to encode 12 different transcripts produced by alternative splicing of the first exon, which contains a large portion of the 5′ untranslated region (UTR) of the *cpx* mRNA, but no coding sequence. Alternative splicing of the first exon is well supported by sequences of ESTs that correspond to those found in the alternate first exons. In general, the 5′ UTR of mRNA sequences can regulate both translation initiation and mRNA stability (Pickering and Willis, 2005). The wide variety of 5′ UTRs in *cpx* transcripts suggests that the timing, level, and/or location of Cpx expression is likely to be tightly regulated in *Drosophila*. We also identified alternative splicing that altered coding exons within Cpx. Notably, the far C-terminus is encoded by one of two alternatives for exon 7, which we term exon 7A and exon 7B. We PCR amplified and sequenced individual cDNAs from the ATG start site in exon 3 to the stop codon in exon 7A or exon 7B. Although alternative splicing

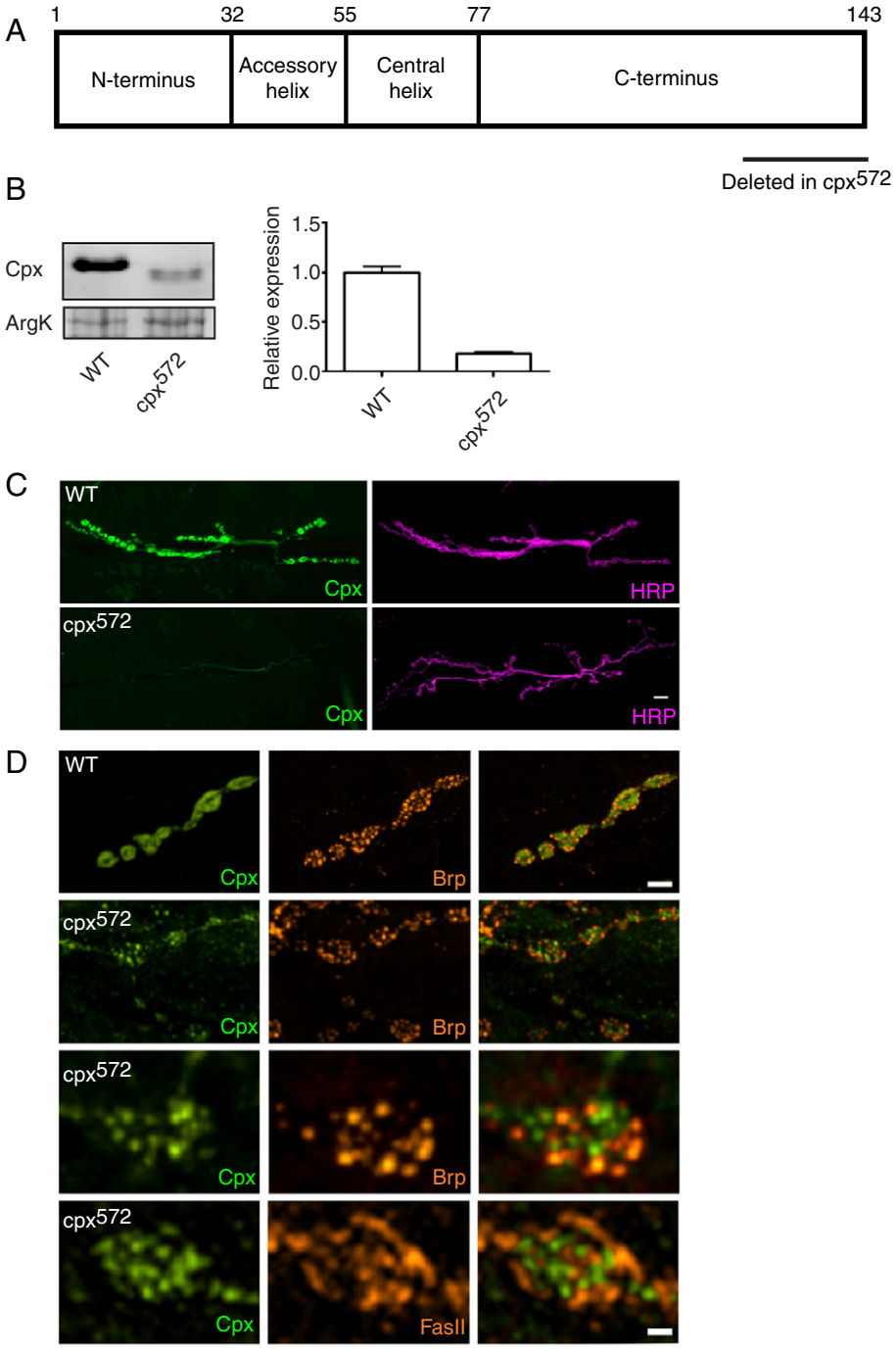

Fig. 1. The complexin C-terminus is necessary for protein stability and localization. (A) Diagram showing subdomains of the Cpx protein as first reported by Xue et al. (2007). The numbering corresponds to residues in DmCpx7A. The region of the C-terminus deleted in *cpx*^{572} mutants is indicated. (B) Western blot analysis of Cpx protein levels in *cpx*^{572} mutants. Bands corresponding to Cpx and the loading control arginine kinase (ArgK) are shown for Canton S (wildtype — WT) and *cpx*^{572} mutant animals. Note the truncated Cpx protein product in *cpx*^{572} mutants. The Cpx expression level was normalized to wildtype. (C) Staining of 3rd instar larval muscle 6/7 NMJs from segment A3 with antibodies against horseradish peroxidase (HRP) and Cpx indicated reduced Cpx immunoreactivity in synaptic boutons in *cpx*^{572} mutants. Scale bar = 10 μm. (D) Wildtype Cpx distributes uniformly over the bouton periphery and nonspecifically overlaps with the active zone protein Bruchpilot (Brp, top panel). Higher intensity imaging reveals that the truncated protein in *cpx*^{572} animals localizes to punctuated structures that reside near, but do not completely overlap, active zones labeled by anti-BRP (middle panels). Similarly, truncated Cpx does not overlap with the peri-active zone marker, Fas II (bottom panel). Scale bar is 5 μm for the top two panels and 1 μm for the bottom two panels.

was predicted for exon 4, only exon 4B (Fig. 3A) was ever found from a total of 70 sequenced cDNAs, and alternative splicing of exon 5 resulted in the insertion of only a single amino acid for transcripts utilizing exon 5A compared to exon 5B. By far the most extensive sequence variation occurred due to alternative splicing of exons 7A and 7B, encoding the final 24 and 20 residues, respectively, in the far C-terminus of Cpx. Hereafter, the most abundant transcripts utilizing exon 7A and exon 7B will be referred to as DmCpx7A and DmCpx7B, respectively.

The C-terminus of Cpx is not highly conserved from invertebrates to mammals, particularly in the far C-terminus encoded by exon 7 in DmCpx (Fig. 3B). However, DmCpx7A contains a C-terminal CAAX-box, similar to mammalian Cpx 3 (mCpx3) and mCpx4, which allows for post-translational prenylation by the addition of either

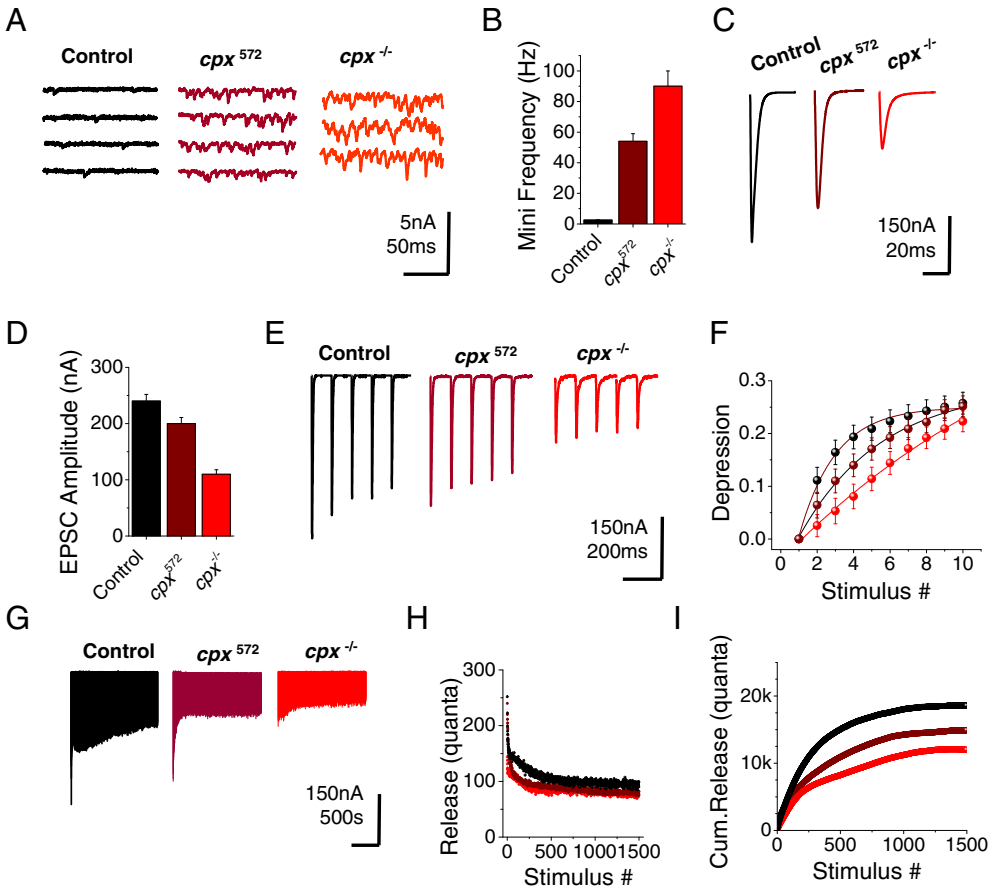

Fig. 2. Synaptic defects in animals lacking the complexin C-terminus. (A) Postsynaptic current recordings of spontaneous release at muscle 6 NMJs in control (black), cpx^{572} (brown) and $cpx^{-/-}$ (cpx^{SH1} — red). This genotypic color code is maintained throughout the figure. (B) Quantification of average spontaneous release rate revealed significant difference between control and cpx^{572} ($p<0.001$), between control and $cpx^{-/-}$ ($p<0.001$), and between cpx^{572} and $cpx^{-/-}$ ($p<0.001$). (C) Representative EPSCs in control, cpx^{572} and $cpx^{-/-}$ in 2.0 mM external Ca^{2+} saline. (D) Quantification of average EPSC amplitude revealed significant difference between control and cpx^{572} ($p<0.01$), between control and $cpx^{-/-}$ ($p<0.001$), and between cpx^{572} and $cpx^{-/-}$ ($p<0.001$). (E) Representative EPSCs during a brief period of stimulation at 10 Hz in control, cpx^{572} and $cpx^{-/-}$. (F) Quantification of average synaptic depression (1-$EPSC_t$/EPSC) observed during a 10 Hz stimulation. The time course of depression revealed significant differences between control and cpx^{572} ($p<0.01$), between control and $cpx^{-/-}$ ($p<0.001$), and between cpx^{572} and $cpx^{-/-}$ ($p<0.01$). (G) Representative EPSCs during a longer stimulation (1500 stimuli) at 10 Hz in control, cpx^{572} and $cpx^{-/-}$. (H) Average quantal content during the long tetanus in control, cpx^{572} and $cpx^{-/-}$. (I) Cumulative release during a 10 Hz stimulation train revealed a reduction in released quanta in cpx^{572} synapses compared to control ($p<0.01$), in cpx^{572} synapses compared to $cpx^{-/-}$ ($p<0.01$) and in $cpx^{-/-}$ synapses compared to control ($p<0.01$). Equation: $y=A1*\exp(-x/t1)+y0$, Chi^2/DoF = 0.00004, R^2 = 0.99617, $y0=0.750\pm0.004$, $A1=0.245\pm0.006$, $t1=2.0\pm0.13$, $y0\_2=0.453\pm0.139$, $A1\_2=0.553\pm0.136$, $t1\_2=16.3\pm5.3$, $y0\_3=0.71\pm0.01$, $A1\_3=0.28\pm0.0108$, $t1\_3=4.50\pm0.44$. All experiments were performed in 0.2 mM external Ca^{2+} solution. The data represent the mean responses in at least six different animals for each genotype for all panels. Error bars, SEM.

a farnesyl (15-carbon chain) or geranylgeranyl (20-carbon chain) moiety to the cysteine residue and elimination of the terminal three amino acids (Zhang and Casey, 1996). Prenylation can mediate membrane association and protein–protein interactions (Zhang and Casey, 1996), and this CAAX-box is implicated in proper localization of DmCpx7A, mCpx3 and mCpx4 (Cho et al., 2010; Reim et al., 2005; Xue et al., 2009). DmCpx7B lacks a C-terminal CAAX-box, similar to mCpx1 and mCpx2. The unique exon expressed by DmCpx7B is highly conserved among 10 related *Drosophila* species (data not shown), indicating evolutionary pressure to maintain both isoforms of Cpx. These results suggest that although *Drosophila* encodes only a single *Cpx* gene, alternative splicing generates functional variants that contain or lack a CAAX-box, similar to mammalian Cpxs.

To determine expression differences between DmCpx7A and DmCpx7B, we designed primers specific for exon 7A or exon 7B and used quantitative RT-PCR to calculate the relative abundance of DmCpx7A and DmCpx7B transcripts. Among both adult and larval transcripts, DmCpx7A was ~1000-fold more abundant than DmCpx7B (Fig. 3C), suggesting that DmCpx7A is the predominant isoform and that alternative splicing of exon 7 is not developmentally regulated at the time points studied. We also examined whether the relative abundance of DmCpx7A or DmCpx7B was regulated by neuronal activity using a previously reported approach with the temperature-sensitive mutants *paralytic* ($para^{TS1}$) and *seizure* (sei^{TS1}) (Guan et al., 2005). sei^{TS1} is a hyperactivity mutant that disrupts an ERG potassium channel that functions in action potential repolarization. $para^{TS1}$ mutants have reduced neuronal excitability secondary to dysfunction in the voltage-gated sodium channel. Total RNA samples were prepared from $para^{TS1}$ and sei^{TS1} adults following different heat shock protocols to mimic neuronal hypoactivity and hyperactivity, respectively. In the acute heat shock protocol, animals were given a 20-min heat shock at 37 °C followed by a 30-min recovery period. In the chronic heat shock protocol, animals were given four 5-min heat shocks at 37 °C spaced 1 h apart and followed by a 24-hour recovery period. At baseline without heat shock, both DmCpx7A and DmCpx7B levels were elevated in sei^{TS1} mutants ($p<0.01$ and $p<0.001$, respectively, two-way ANOVA Bonferroni post-test) and DmCpx7B levels were reduced in $para^{TS1}$ mutants ($p<0.001$) compared to wild-type controls. There was no difference in the activity-dependence of DmCpx7A vs. DmCpx7B ($p>0.05$, two-way ANOVA; Fig. 3D). However, both transcripts were significantly downregulated in sei^{TS1} mutants following the acute or chronic heat shock protocols vs. untreated sei^{TS1} animals

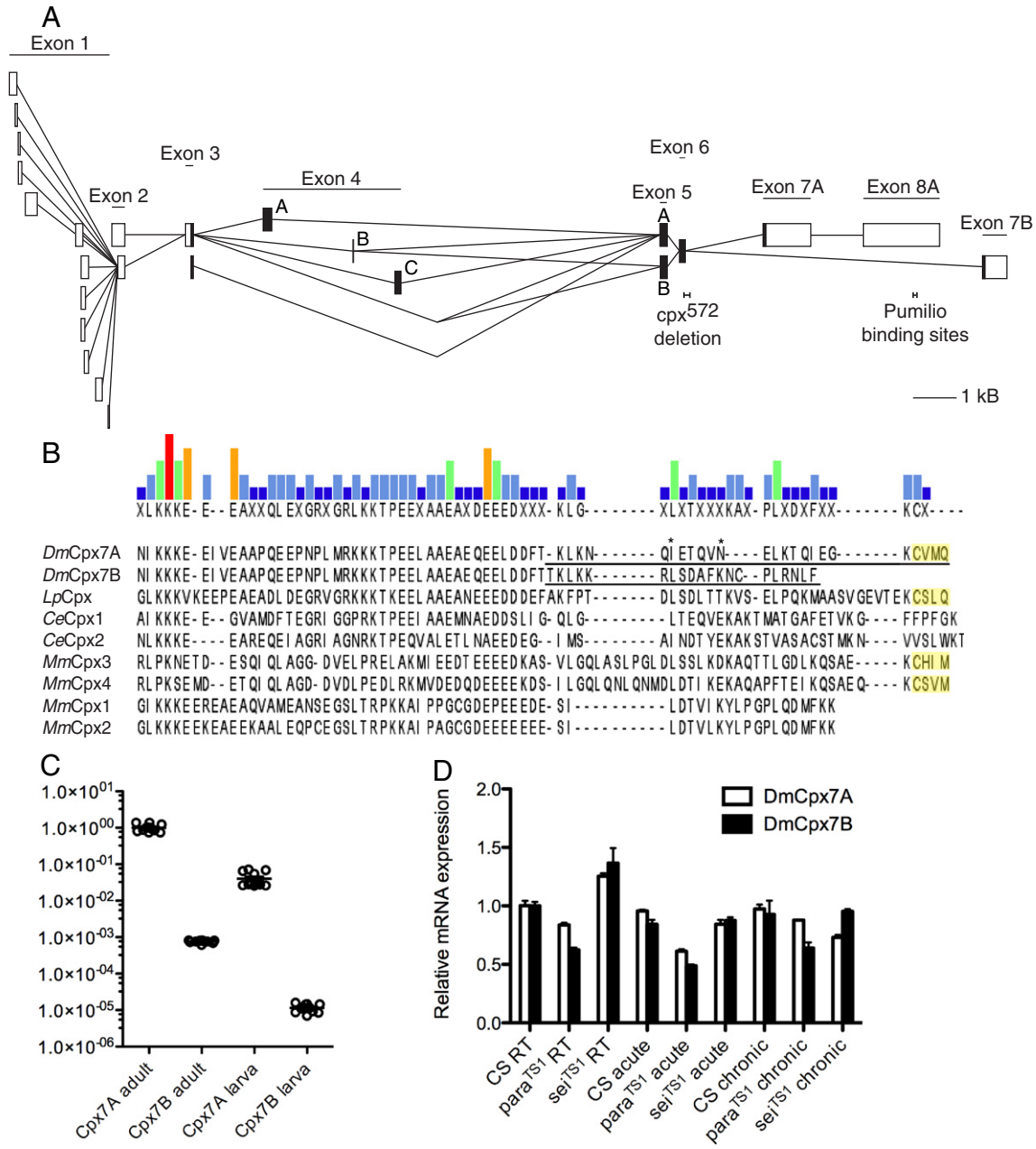

Fig. 3. The *Drosophila Cpx* locus generates multiple splice isoforms. (A) Scale diagram indicating alternative splice variants of Cpx. Protein-coding regions are shaded. The genomic deletion in cpx^{572} mutants and Pumilio binding sites in exon 8A are indicated. (B) Alignment of the C-termini of Cpxs from several species. Alignment was generated using the ClustalW algorithm with MegAlign software (DNASTAR). C-terminal prenylation motifs are highlighted in yellow. The regions of DmCpx7A and DmCpx7B encoded by exon 7 are underlined, and the residues in exon 7A subject to RNA editing are indicated with an asterisk. The consensus sequence is shown at the top, and the level of conservation of each residue is indicated by the height of the bar. Species abbreviations: Dm — *Drosophila melanogaster*, Lp — *Loligo pealeii* (squid), Ce — *Caenorhabditis elegans*, Mm — *Mus musculus*. (C) Log-scale graph of quantitative RT-PCR results indicating the expression levels of DmCpx7A and DmCpx7B transcripts in adult flies and 3rd instar larvae. All values were normalized to the expression level of DmCpx7A in adult flies. (D) Graph of quantitative RT-PCR results indicating the expression levels of DmCpx7A and DmCpx7B transcripts in adult flies of the indicated genotype and heat shock protocol. RT — room temperature (no heat shock); acute — 30-min recovery after a 20-min heat shock at 37 °C; chronic — 24-hour recovery following four 5-min heat shocks at 37 °C spaced 1 h apart. There was no difference in the activity-dependence of DmCpx7A vs. DmCpx7B ($p > 0.05$, two-way ANOVA). However, both transcripts were significantly downregulated in sei^{TS1} mutants following the acute or chronic heat shock protocols vs. untreated sei^{TS1} animals ($p < 0.001$, two-way ANOVA Bonferroni post-test).

($p < 0.001$, two-way ANOVA Bonferroni post-test). In summary, our results suggest that neuronal activity levels can modulate Cpx mRNA expression, potentially altering basal release properties of the synapse in an activity-dependent manner.

RNA editing of the DmCpx7A C-terminus generates four unique isoforms

In addition to alternative splicing, DmCpx expression can be regulated post-transcriptionally by RNA editing. Hoopengardner et al. (2003) used a comparative genomics approach with 18 *Drosophila* species to identify targets of the RNA editing enzyme adenosine deaminase acting on RNA (ADAR) and found three sites of RNA editing within DmCpx exon 7A: position 375, which encodes isoleucine (Ile) residue 125, and positions 388 and 389, which encode asparagine (Asn) residue 130. RNA editing at position 375 changes Ile-125 to methionine (Met), and RNA editing at positions 388 and 389 can change Asn-130 to aspartate (Asp), serine (Ser) or glycine (Gly). The amino acid possibilities at residue 130 are intriguing

as Asp is phospho-mimetic, Ser is phospho-competent and Gly is phospho-incompetent, raising the possibility that phosphorylation at this site may regulate DmCpx7A function. The ADAR enzymes require a double-stranded RNA substrate, which is usually provided by an imperfect duplex in the pre-mRNA formed by base pairing between the exon containing the adenosine(s) to be edited and an intronic region called the editing site complementary sequence (ECS) (Higuchi et al., 1993). To investigate the occurrence of RNA editing in DmCpx exon 7A, we compared intronic sequences from 12 *Drosophila* species to identify highly conserved regions that could function as the ECS. A region of near perfect conservation was found in the final 65 bp of intron 6 extending through the first 88 bp of exon 7A (Fig. 4A). The mfold algorithm for prediction of RNA secondary structure (Zuker, 2003) suggests that this region folds into an extended, imperfect RNA duplex (Fig. 4B), satisfying the requirements for an ADAR substrate.

To determine the extent of RNA editing of *Cpx* in *Drosophila*, we sequenced individual cDNA segments of the editing region amplified by RT-PCR. Interestingly, editing was never observed at the second and third sites (A388, A389) unless editing had also occurred at the first site (A375). According to the mfold algorithm, editing at A375 is predicted to extend the length of the imperfect RNA duplex (Fig. 4C), making it a potentially more stable or attractive substrate for ADAR to carry out editing at sites A388 and A389. At these final two sites, editing was either observed at A389, giving rise to a Ser at residue 130, or at both A388 and A389, giving rise to a Gly at residue 130, but not at A388 alone. Thus, we identified four RNA editing isoforms of DmCpx exon 7A in vivo: Ile125/Asn130 (the unedited isoform), Met125/Asn130, Met125/Ser130, and Met125/Gly130. As a percentage of 96 individual cDNAs sequenced, each isoform was represented as follows: Ile125/Asn130 = 61.5%, Met 125/Asn130 = 7.3%, Met125/Ser130 = 10.4%, and Met125/Gly130 = 20.8%. Only a small subset of transcripts is known to be RNA edited, and nearly all encode proteins involved in rapid neurotransmission (Hoopengardner et al., 2003). Although it is unclear how editing alters Cpx function, mRNA sequencing indicates multiple isoforms of the edited protein are likely to be present at synapses that could differentially impact release properties.

DmCpx7A and DmCpx7B show similar localization and mobility at the larval NMJ

Given that cpx^{572} mutants showed defects in Cpx localization at synaptic boutons, we sought to determine whether DmCpx7A and DmCpx7B might display differential localization at synapses due to their highly divergent C-termini. We first carried out in situ hybridization analysis of late-stage embryos to determine their expression pattern. Antisense hybridization probes specific for DmCpx7A and DmCpx7B were designed from the 3′ untranslated regions of exon 7A and exon 7B, respectively. Both DmCpx7A and DmCpx7B showed clear expression in the developing central nervous system and ventral nerve cord (Fig. 5A). Consistent with the RT-PCR results, the DmCpx7A signal was more robust than that of DmCpx7B. These results suggest that both DmCpx7A and DmCpx7B are expressed in the developing nervous system without an obvious region-specific distribution.

We next looked at transgene expression at the larval NMJ. As we were unable to generate antisera specific to DmCpx7A and DmCpx7B, we turned to the Gal4-UAS system (Brand and Perrimon, 1993). We generated transgenic animals expressing DmCpx7A or DmCpx7B mRNAs downstream of a UAS sequence. When driven pan-neuronally with the $elav^{C155}$-Gal4 driver in the *cpx* null background (cpx^{SH1}), robust expression of both DmCpx7A and DmCpx7B was observed in synaptic boutons at the larval NMJ by immunostaining with a pan-Cpx antiserum (Huntwork and Littleton, 2007) (Fig. 5B). The halo-shaped distribution of both transgenic proteins was reminiscent of synaptic vesicle-associated proteins such as Syt 1 (Littleton et al., 1993). We next co-expressed DmCpx7A and DmCpx7B transgenic proteins tagged with either GFP or mCherry with the $elav^{C155}$-Gal4 driver in the *cpx* null background (cpx^{SH1}). Both proteins showed similar subcellular distribution within presynaptic boutons (Fig. 5C), suggesting that either isoform of the protein can target effectively to synaptic terminals.

In transfected neurons, prenylation of mCpx3 and mCpx4 results in a distinct distribution from that of mCpx1 and mCpx2, which lack prenylation (Reim et al., 2005). mCpx3 and mCpx4 appear to be concentrated around synaptic terminals, whereas mCpx1 and mCpx2 are distributed more diffusely throughout axonal processes. Although DmCpx7A, which contains a prenylation motif, and DmCpx7B, which lacks a prenylation motif, showed similar localization at the larval NMJ at the level of confocal microscopy, we wondered whether prenylation of DmCpx7A might result in membrane targeting to synaptic vesicles or the synaptic plasma membrane that would alter its mobility compared to DmCpx7B. We generated N-terminal GFP-tagged DmCpx7A and DmCpx7B transgenic animals and used fluorescence recovery after photobleaching (FRAP) to follow the dynamics of the two Cpx isoforms at synapses. As a control, we used animals expressing UAS-GFP alone to compare to dynamics of soluble

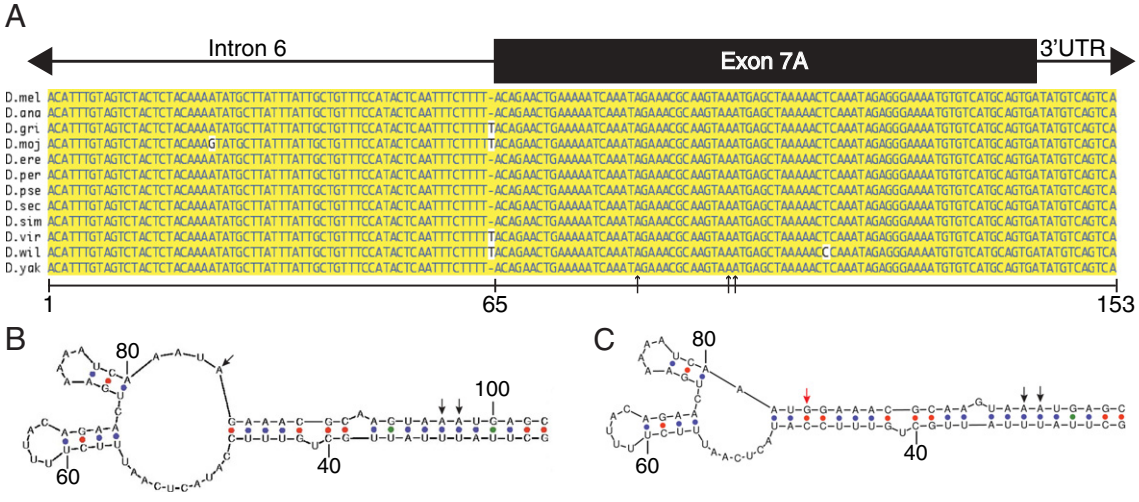

Fig. 4. RNA editing alters the C-terminus of DmCpx7A. (A) Alignment of an almost perfectly conserved region of Cpx intron 6 and exon 7 among 12 *Drosophila* species. The three sites of RNA editing in exon 7A are indicated with arrows. (B–C) Predicted RNA secondary structure of the region shown in A based on the mfold algorithm (Zuker, 2003) before (B) and after (C) editing of the first site (A375), indicated by the red arrow in C.

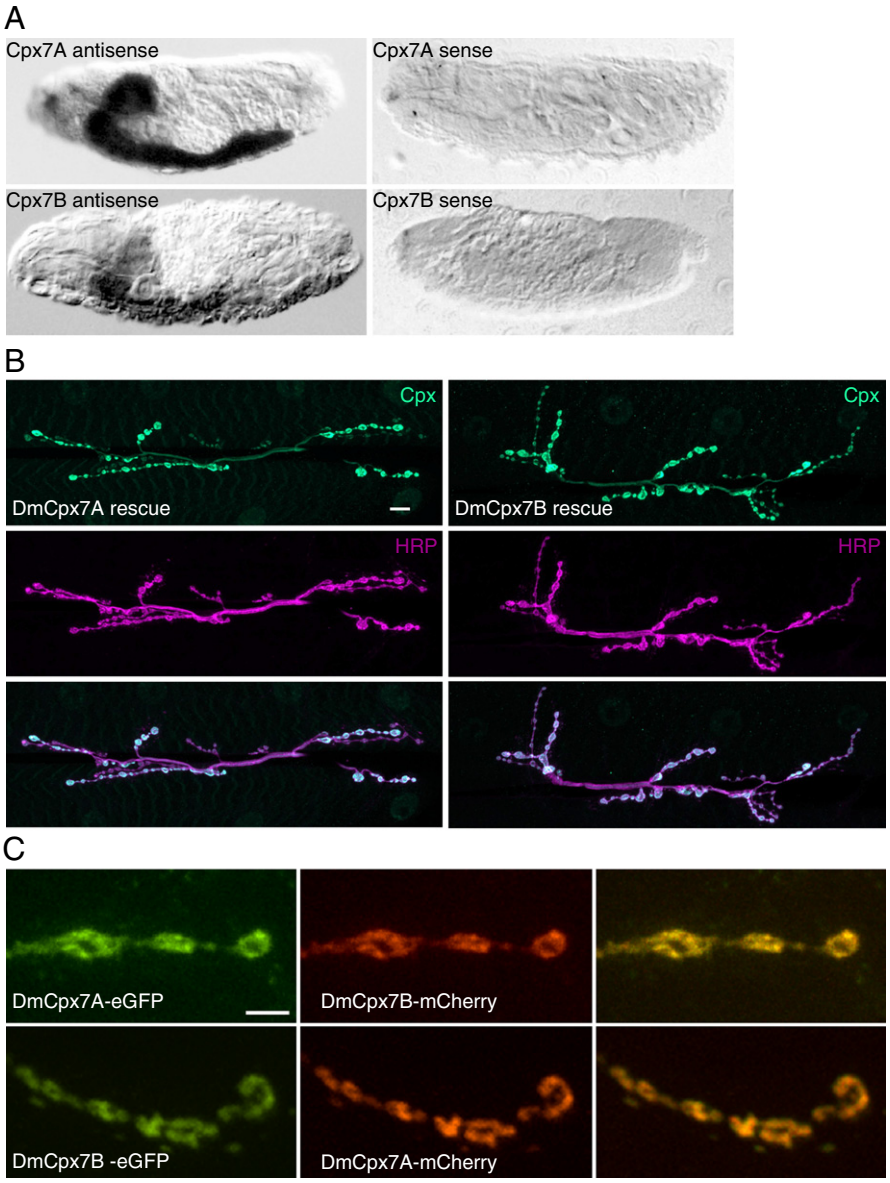

Fig. 5. DmCpx7A and DmCpx7B have similar expression patterns in the developing nervous system and at the NMJ. (A) Lateral view of in situ hybridization on late stage embryos with DmCpx7A and DmCpx7B cRNA probes. Sense cRNA probes are shown as negative controls. (B) Staining of 3rd instar larval muscle 6/7 NMJs from segment A3 with antibodies against horseradish peroxidase (HRP) and Cpx showing similar Cpx immunoreactivity in DmCpx7A and DmCpx7B rescue animals (*elav*^{C155}-Gal4;;*cpx*^{SH1}, UAS-DmCpx). Scale bar = 10 μm. (C) Co-expression of DmCpx7A-eGFP and DmCpx7B-mCherry (top panel) or DmCpx7A-mCherry and DmCpx7B-eGFP (bottom panel) at 3rd instar NMJs in *cpx* null mutants with *elav*^{C155}-Gal4.

proteins, and UAS-Synaptogyrin-GFP to compare the dynamics of synaptic vesicle proteins. We selected large diameter synaptic boutons at muscle fiber 6 and used FRAP to photobleach half of the bouton. We then followed recovery of the GFP-tagged proteins into the bleached area for 1 min in 10-second intervals using a Perkin Elmer spinning disk confocal microscope. Quantitative analysis of FRAP recovery revealed that GFP-tagged DmCpx7A and DmCpx7B behaved similarly, with a slower diffusion rate than cytosolic GFP alone, but faster than the synaptic vesicle membrane-tethered Synaptogyrin-GFP (Fig. 6A, B). We conclude that both Cpx isoforms are highly dynamic within individual synaptic boutons. If DmCpx7A is associated with synaptic vesicles or the plasma membrane via prenylation, our data indicate it can cycle on and off, resulting in faster recovery dynamics than integral membrane synaptic vesicle proteins. Alternatively, a significant population of Cpx7A might lack prenylation altogether.

DmCpx7A and DmCpx7B differentially regulate spontaneous and evoked neurotransmitter release

To evaluate functional differences between DmCpx7A and DmCpx7B, we tested the ability of the transgenes to rescue the synaptic transmission defects of *cpx* null mutants (*cpx*^{SH1}) when expressed pan-neuronally. *cpx* null mutants alone have a dramatic elevation of spontaneous release and a reduced evoked response (Figs. 2, 7). DmCpx7A fully rescued the elevated mini frequency of *cpx*^{SH1} mutants, whereas DmCpx7B was only partially able to clamp spontaneous fusion (control: 2.5 ± 0.3 Hz, cpx^{SH1}: 80.0 ± 5.0 Hz, DmCpx7A rescue: 3.5 ± 0.3 Hz, DmCpx7B rescue: 10.0 ± 1.0 Hz) (Fig. 7A, B). We compared the ability of DmCpx7A and DmCpx7B to rescue spontaneous release with their putative mammalian (mouse) counterparts that are prenylated like the 7A isoform (mCpx4) or lack a prenylation motif like the 7B isoform (mCpx1). Similar to the effects of the prenylated DmCpx7A isoform,

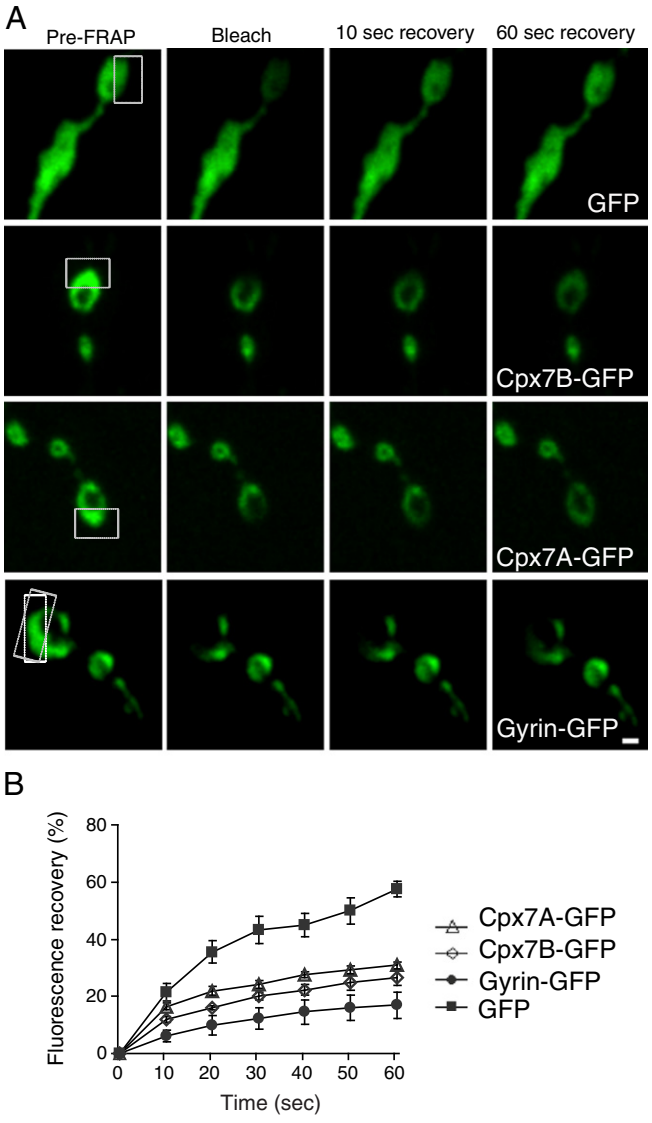

Fig. 6. DmCpx7A and DmCpx7B show similar mobility within NMJ boutons. (A) To determine the rate of diffusion of DmCpx7A-GFP and DmCpx7B-GFP within boutons, FRAP was performed on half the diameter of an individual synaptic bouton (boxed area) to assay intra-synaptic Cpx mobility. The recovery into the bleached area was measured and compared to that of soluble GFP and synaptic vesicle tethered Synaptogyrin-GFP (Gyrin-GFP). Two post-bleaching points at 10 and 60 s are shown for each experiment. Scale bar = 1 μm. (B) Quantitative analysis of fluorescence recovery over time indicates that DmCpx7A and DmCpx7B diffuse slower than soluble GFP, but faster than the synaptic vesicle protein Synaptogyrin. The data represent the mean responses from 7 NMJs in 4 animals for DmCpx7A, 8 NMJs from 4 animals for DmCpx7B, 12 NMJs from 4 animals for GFP alone, and 10 NMJs from 5 animals for Gyrin-GFP. Error bars, SEM.

mCpx4 was able to robustly rescue the enhanced spontaneous fusion rate to control levels (Fig. 7A, B). In contrast, the unprenylated mCpx1 isoform failed to fully rescue the enhanced spontaneous release, similar to DmCpx7B. These results indicate a functional diversification of the *Drosophila* splice variants with respect to clamping properties, similar to what has been achieved with gene duplication in mammals. To further examine differences in DmCpx7A and DmCpx7B, we measured evoked neurotransmitter release in transgenically rescued animals expressing either isoform. DmCpx7A was able to rescue the reduced amplitude of EJCs of cpx^{SH1} mutants, whereas DmCpx7B showed a strong enhancement of EJC amplitude that is more than twice to that seen in controls (control: 6.5 ± 0.7 nA, cpx^{SH1}: 4.0 ± 0.3 nA, DmCpx7A rescue: 7.2 ± 0.7 nA, DmCpx7B rescue: 16.0 ± 1.5 nA) (Fig. 7C).

We next compared the rescue of evoked responses by the *Drosophila* splice isoforms to that achieved with mCpx1 and mCpx4. We observed that mCpx4 again behaved similarly to DmCpx7A, rescuing the evoked defect in cpx^{SH1} mutants (Fig. 7C). In contrast, mCpx1 behaved like DmCpx7B, enhancing evoked release to far greater levels than controls (Fig. 7C), similar to previous observations (Cho et al., 2010). We conclude that DmCpx7A is a better inhibitor of spontaneous release, while DmCpx7B is a better facilitator of evoked neurotransmitter release. These properties are similar to the rescue effects observed for the prenylated (mCpx4) and unprenylated (mCpx1) mammalian isoforms in our model. A number of reports have suggested that Cpx has different effects on spontaneous vs. evoked neurotransmitter release (Cho et al., 2010; Hobson et al., 2011; Huntwork and Littleton, 2007; Martin et al., 2011; Maximov et al., 2009). Our data indicate that the C-terminus of *Drosophila* Cpx regulates both spontaneous and evoked fusion, and that alternative splicing generates isoforms with distinct effects on the two release mechanisms.

Discussion

Although SNAREs make up the core fusion machinery in all cells, additional SNARE-associated proteins are required for rapid Ca^{2+}-mediated neurotransmitter release at synapses. Along with the vesicular Ca^{2+} sensor Syt 1, Cpx has emerged as a key regulator of SNARE-mediated fusion. By binding to assembled neuronal SNARE complexes with 1:1 stoichiometry, Cpx is ideally situated to regulate vesicle fusion, but its precise role remains unclear. Initial genetic studies in mice and *Drosophila* suggested opposing functions in evoked versus spontaneous release (Huntwork and Littleton, 2007; Xue et al., 2008), and in vitro studies of fusion driven by SNAREs and Cpx gave mixed results (Giraudo et al., 2006; Malsam et al., 2009; Schaub et al., 2006; Seiler et al., 2009). Genetic knock-outs of mCpx 1, 2 and 3 resulted in a reduction in both mini frequency and evoked neurotransmitter release in hippocampal autaptic cultures, suggesting a facilitatory role for Cpx in synaptic vesicle fusion. Genetic analysis of the single *Cpx* gene in *Drosophila* revealed a dramatic increase (>40-fold) in mini frequency and a reduction in evoked neurotransmitter release at the larval NMJ, suggesting that Cpx has different effects on these two modes of synaptic vesicle fusion.

More recent studies using RNAi knock-down of Cpxs in mouse cortical cultures (Maximov et al., 2009) and genetic knock-outs of Cpx-1 at the *C. elegans* NMJ (Hobson et al., 2011; Martin et al., 2011) found similar results to the original *Drosophila* study (Huntwork and Littleton, 2007), supporting a model in which Cpx inhibits spontaneous vesicle fusion and promotes synchronous evoked vesicle fusion. What distinguishes these two modes of vesicle fusion at the molecular level, however, remains unclear. Structure–function studies of Cpx (Giraudo et al., 2009; Hobson et al., 2011; Martin et al., 2011; Xue et al., 2007, 2009, 2010) have indicated the presence of opposing inhibitory and facilitatory subdomains in the N-terminus of the protein. It has been suggested that the facilitatory and inhibitory functions of the Cpx N-terminus may be weighted differently depending on the model system and synapse examined (Xue et al., 2009), explaining some of the divergent results regarding the effect of Cpx on spontaneous release. The role of the C-terminus, however, is less clear. In vitro, the C-terminus of mCpx1 appears to inhibit SNARE-mediated cell–cell fusion (Giraudo et al., 2008), but promotes SNARE-mediated liposome fusion (Malsam et al., 2009). On the other hand, Cpx constructs lacking the C-terminus are functional in hippocampal autaptic culture (Xue et al., 2007), but fail to rescue the aldicarb sensitivity of *cpx-1* null mutants in *C. elegans* (Martin et al., 2011). Finally, lentiviral rescue of shRNAi mCpx1/mCpx2 knockdown cultured cortical neurons indicated that the Cpx C-terminus regulated clamping and vesicle priming functions of the protein, but not Ca^{2+}-triggering of evoked release (Kaeser-Woo et al., 2012). These results suggest that the C-terminus

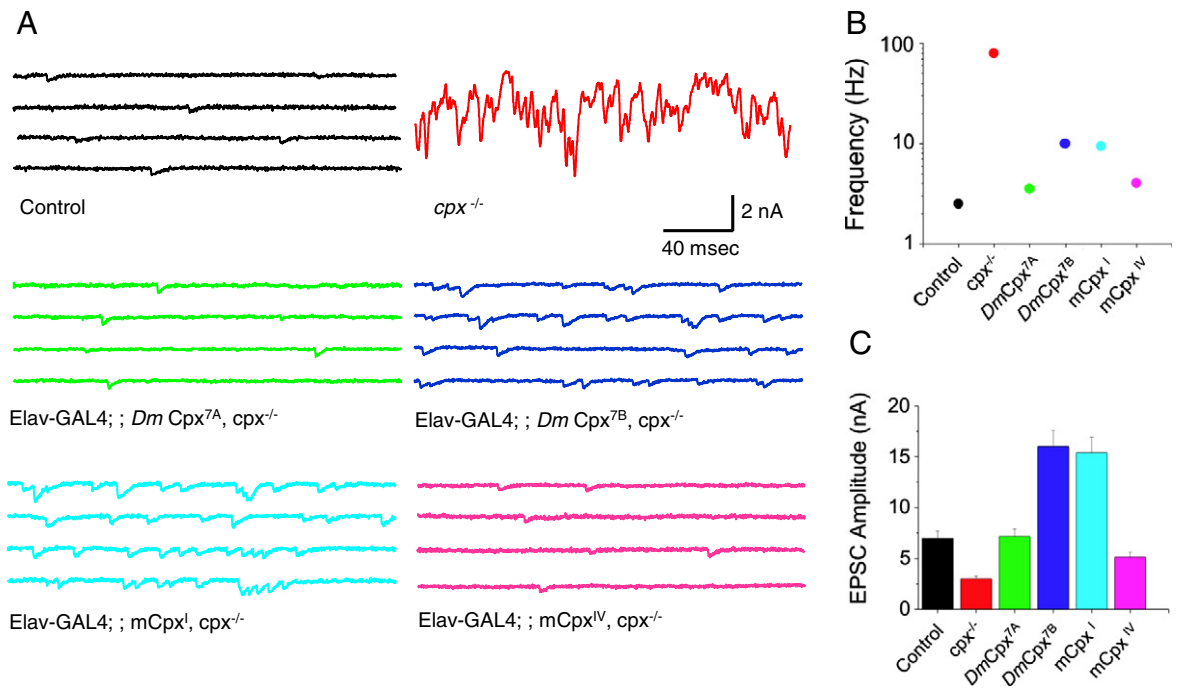

Fig. 7. DmCpx splice variants and orthologous mammalian isoforms share similar clamping properties. (A) Postsynaptic current recordings of spontaneous release at muscle 6 synapses in control (black), $cpx^{-/-}$ null mutants (red), Elav-GAL4;; *DmCpx7A*, $cpx^{-/-}$ (green), Elav-GAL4;; *DmCpx7B*, $cpx^{-/-}$ (blue), Elav-GAL4;; mCpxI, $cpx^{-/-}$ (aqua), and Elav-GAL4;; mCpxIV, $cpx^{-/-}$ (magenta). (B) Quantification of average mini frequency in each condition on a semi-logarithmic plot. Mean mini frequencies in the genotypes are: control: 2.5±0.2 Hz; $cpx^{-/-}$: 80.6±5 Hz; Elav-GAL4;; *DmCpx7A*, $cpx^{-/-}$: 3.5±0.4 Hz; Elav-GAL4;; *DmCpx7B*, $cpx^{-/-}$: 10±1.1 Hz; Elav-GAL4;; mCpxI, $cpx^{-/-}$: 9.4±0.9 Hz; Elav-GAL4;; mCpxIV, $cpx^{-/-}$: 4.0±0.4. Student's t-test revealed significant differences between control and $cpx^{-/-}$ ($p<0.001$); control and Elav-GAL4;; *DmCpx7B*, $cpx^{-/-}$ ($p<0.01$); control and Elav-GAL4;; mCpxI, $cpx^{-/-}$ ($p<0.01$); $cpx^{-/-}$ and Elav-GAL4;; *DmCpx7A*, $cpx^{-/-}$ ($p<0.01$); $cpx^{-/-}$ and Elav-GAL4;; *DmCpx7B*, $cpx^{-/-}$($p<0.001$); $cpx^{-/-}$ and Elav-GAL4;; mCpxI, $cpx^{-/-}$ ($p<0.001$); and $cpx^{-/-}$ and Elav-GAL4;; mCpxIV, $cpx^{-/-}$ ($p<0.001$). (C) Quantification of average EPSC amplitude in each condition. Mean EPSC amplitudes in the genotypes are: control: 7.0±0.6 Hz; $cpx^{-/-}$: 3.0±5 Hz; Elav-GAL4;; *Dm Cpx7A*, $cpx^{-/-}$: 7.2±0.7 Hz; Elav-GAL4;; *DmCpx7B*, $cpx^{-/-}$: 16.0±1.5 Hz; Elav-GAL4;; mCpxI, $cpx^{-/-}$: 15.4±1.5; Elav-GAL4;; mCpxIV, $cpx^{-/-}$: 5.1±0.5. Student's t-test revealed significant differences between control and $cpx^{-/-}$ ($p<0.001$); control and Elav-GAL4;; *DmCpx7B*, $cpx^{-/-}$ ($p<0.01$); control and Elav-GAL4;; mCpxI, $cpx^{-/-}$ ($p<0.01$); $cpx^{-/-}$ and Elav-GAL4;; *DmCpx7A*, $cpx^{-/-}$ ($p<0.01$); $cpx^{-/-}$ and Elav-GAL4;; *DmCpx7B*, $cpx^{-/-}$ ($p<0.001$); $cpx^{-/-}$ and Elav-GAL4;; mCpxI, $cpx^{-/-}$ ($p<0.001$); and $cpx^{-/-}$ and Elav-GAL4;; mCpxIV, $cpx^{-/-}$ ($p<0.01$). All experiments were performed in 0.2 mM external Ca^{2+} solution. The data represent the mean responses in at least six different animals for each genotype for all panels. Error bars, SEM.

may exert an effect on neurotransmitter release at some, but not all, synapses.

To address the uncertainty regarding the function of the C-terminus of Cpx, we identified and characterized a *Drosophila* mutant cpx^{572}, which contains an early stop codon that eliminates the final ~25 residues of the C-terminus. These mutants generated a truncated form of Cpx that was present at ~20% of wild type levels in adult head extracts and mislocalized at synaptic boutons at the larval NMJ. In addition, cpx^{572} mutants displayed similar, though slightly milder, defects in synaptic transmission compared to *cpx* null animals. These results argue that the C-terminus of DmCpx is important for protein stability and function. We subsequently examined naturally occurring splice isoforms of DmCpx and identified a splicing event that leads to two alternative far C-termini. These isoforms, DmCpx7A and DmCpx7B, differ in the final ~25 residues of the protein (the same region that is truncated in cpx^{572} mutants). DmCpx7A is the predominant isoform at the mRNA level in both larvae and adults (Fig. 3C), and both DmCpx7A and DmCpx7B transcripts show similar activity dependence in the temperature-sensitive activity mutants $para^{TS1}$ and sei^{TS1} (Fig. 3D). However, the presence of multiple Pumilio binding sites in the 3′ UTR of DmCpx7A, but not DmCpx7B (Fig. 3A), raises the possibility that the translation of these isoforms may undergo additional regulation. In addition, DmCpx7A undergoes RNA editing within exon 7 to generate further diversity. Editing at one of the sites in DmCpx7A generates a potential phosphorylation site within this domain. Like the edited version of DmCpx7A, the DmCpx7B isoform also contains a potential phosphorylation site in exon 7. Future experiments with edited and non-edited transgenes will be required to define how RNA editing of Cpx regulates its effects on neurotransmission.

Based on the altered Cpx protein localization at the larval NMJ in cpx^{572} mutants (Fig. 1C), we hypothesized that DmCpx7A and DmCpx7B would show distinct localization patterns at synapses. Although isoform-specific antisera failed to recognize any Cpx immunoreactivity on fixed tissue, we could detect expression of DmCpx7A and DmCpx7B transgenes using pan-Cpx antiserum (Huntwork and Littleton, 2007) or transgenically expressed fluorescently-tagged variants. At the level of confocal microscopy, both transgenes localized to synaptic boutons at the larval NMJ in a halo pattern (Fig. 5B) reminiscent of synaptic vesicle-associated proteins such as Syt 1 (Littleton et al., 1993). These data indicate that although the far C-terminus of Cpx is necessary for proper protein localization, the dissimilar C-terminal sequences of DmCpx7A and DmCpx7B both allow for trafficking to synapses. We also performed FRAP analysis of GFP-tagged DmCpx7A and DmCpx7B GFP-tagged proteins at individual synapses. Both proteins were highly mobile within bleached boutons, recovering faster than a synaptic vesicle integral membrane protein, but slower than cytoplasmic GFP (Fig. 6).

Finally, we examined the function of DmCpx7A and DmCpx7B in synaptic transmission at the larval NMJ by expressing the transgenes in a *cpx* null mutant background (cpx^{SH1}) and evaluating their ability to rescue the elevated mini frequency and decreased evoked neurotransmitter release observed in cpx^{SH1} mutants (Huntwork and Littleton, 2007). DmCpx7A was able to restore control levels for both mini frequency and evoked neurotransmitter release (Fig. 7A–B). In contrast,

DmCpx7B only partially rescued the elevated mini frequency but promoted evoked neurotransmitter release to more than twice the levels of control (Fig. 7A–B). A number of studies have shown distinct roles for Cpx in spontaneous vs. evoked neurotransmitter release. Besides the increased mini frequency and reduced evoked neurotransmitter release observed in *Drosophila cpx* mutants, similar results have now been reported at the *C. elegans* NMJ (Hobson et al., 2011; Martin et al., 2011). In mice, knockouts of mCpx 1, 2 and 3 show decreases in both spontaneous and evoked neurotransmitter release in hippocampal autaptic cultures and certain synapses in brain slices (Xue et al., 2008). In contrast, RNAi knock-down of mCpx 1 and 2 results in increased spontaneous and decreased evoked neurotransmitter release in cortical cultures (Maximov et al., 2009), similar to findings at the *Drosophila* larval and *C. elegans* NMJs. Thus, the emerging trend is that Cpx can have distinct effects on different modes of neurotransmitter release. Our findings with DmCpx7A and DmCpx7B indicate that the differential ability to inhibit spontaneous neurotransmitter release and promote evoked neurotransmitter release can be regulated by the far C-terminus of Cpx.

The most striking difference between the two far C-terminal DmCpx isoforms is the presence of a prenylation motif in DmCpx7A that is absent from DmCpx7B. In mammals, this motif is found in mCpx 3 and 4, but not in mCpx 1 and 2 (McMahon et al., 1995; Reim et al., 2005), and it has been shown to be important for Cpx protein localization (Reim et al., 2005) and function (Cho et al., 2010; Xue et al., 2009). The prenylation motif in mCpx 3 and 4 is necessary for concentrated expression of these proteins near sites of synaptic vesicle release in transfected neurons, and mutations in this motif result in a more diffuse distribution of mCpx 3 and 4, similar to that seen for mCpx 1 and 2, which lack a prenylation motif (Reim et al., 2005). Furthermore, our lab and others have shown that the prenylation motif in DmCpx7A is critical for its function in neurotransmitter release (Cho et al., 2010). Xue et al. (2009) found that mutating the DmCpx7A prenylation motif impaired its ability to inhibit spontaneous neurotransmitter release in hippocampal autaptic cultures. Similarly, Cho et al. (2010) showed that replacing the prenylation motif of DmCpx7A with the final four residues of mCpx1 not only blocked its ability to inhibit spontaneous neurotransmitter release, but also enhanced its ability to promote evoked neurotransmitter release. In short, disrupting the C-terminal prenylation motif of DmCpx7A caused it to function like DmCpx7B. In addition, the differential effects of rescue on evoked and spontaneous release by DmCpx7A and DmCpx7B were similar to those observed for their mammalian counterparts that were prenylated (mCpx4) or not (mCpx1). These data indicate that the far C-terminus, including C-terminal prenylation at the CAAX box, plays a key role in determining how Cpx clamps spontaneous fusion and promotes evoked release.

Based on our *Drosophila* Cpx studies, we propose a model for how DmCpx7A and DmCpx7B might differentially regulate neurotransmitter release (Fig. 8). It has been estimated that three to ten SNARE complexes are needed per vesicle to achieve normal Ca^{2+}-triggered vesicle fusion kinetics (Karatekin et al., 2010; Mohrmann et al., 2010). In contrast, only a single SNARE complex is required for in vitro fusion (van den Bogaart et al., 2010), a process that may more directly apply to random spontaneous minis in vivo. Prenylation of DmCpx7A may tether it to membranes, increasing its local concentration at sites of neurotransmitter release and allowing it to bind to more SNARE complexes per vesicle. To function effectively as a fusion clamp, we hypothesize that Cpx would need to prevent even a single SNARE complex at the synaptic vesicle–membrane interface from exerting fusion-triggering forces. On the other hand, unprenylated DmCpx7B might be present at a lower local concentration at sites of neurotransmitter release. This could lead to binding of DmCpx7B to fewer SNARE complexes per vesicle. If the ability of Cpx to inhibit spontaneous neurotransmitter release were directly correlated to the number of SNARE complexes bound per vesicle, DmCpx7A would be expected to be a stronger fusion clamp than DmCpx7B, as we observe in our rescue experiments (Fig. 7). Several possibilities exist for the enhanced evoked release in DmCpx7B expressing animals. If evoked fusion requires Ca^{2+}-activated Syt 1 to bind to SNARE complexes and displace Cpx, a reduced amount of DmCpx7B attached to SNARE complexes would make it easier for Syt 1 to trigger fusion. Moreover, the ability of Cpx to promote evoked neurotransmitter release has been linked to protein mobility. In vitro, GPI-anchored mCpx 1 was found to inhibit SNARE-mediated cell fusion to a much greater degree than soluble mCpx 1 (Giraudo et al., 2006). More recently, real-time observation of fluorescently labeled Cpx during single evoked exocytic events in PC12 cells showed that Cpx was present only briefly at sites of exocytosis at the onset of fusion. A truncated form of Cpx, however, appeared ~0.5 s prior to the onset of fusion and lingered for ~2 s after fusion, and this longer dwell time was correlated with reduced transmitter release (An et al., 2010). If prenylation of DmCpx7A increased its dwell time at active zone release sites compared to unprenylated DmCpx7B, this might explain why DmCpx7B was better able to promote evoked neurotransmitter release than DmCpx7A in our rescue experiments. In summary, although *Drosophila* contains only one *Cpx*

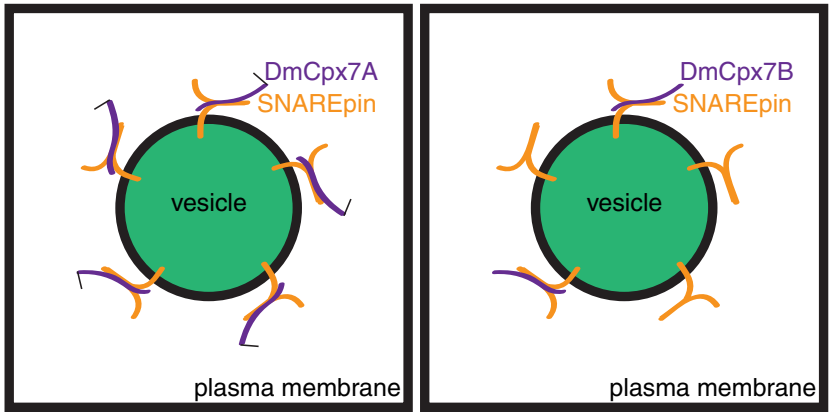

Fig. 8. Model for the differential effects of DmCpx7A and DmCpx7B on neurotransmitter release. A top-down view of a synaptic vesicle fusing with the plasma membrane driven by five SNARE complexes (orange) is shown. Cpx molecules bound to the SNARE complexes are shown in purple, with prenylation of DmCpx7A indicated by a black line. To function as a fusion clamp, we propose that Cpx would need to prevent even a single SNARE complex at the synaptic vesicle–membrane interface from exerting fusion-triggering forces. Prenylation of DmCpx7A may increase its local concentration at sites of fusion and allow it to bind to most SNARE complexes forming during vesicle docking and priming, forming an effective fusion clamp. In contrast, unprenylated DmCpx7B would lack any form of membrane tethering, resulting in a lower local concentration at sites of fusion and a reduction in clamping properties. A reduction in DmCpx7B-bound SNARE complexes might also make it easier for Ca^{2+}-activated Syt 1 to engage SNAREs to trigger fusion by having less Cpx around to compete for SNARE binding.

gene, compared to four *Cpx* genes in mammals, the *DmCpx* locus can produce multiple Cpx isoforms through alternative splicing and RNA editing, perhaps to serve the distinct needs of different synapses. We also demonstrate that alternative splicing of the C-terminus of DmCpx results in two isoforms with differing effects on spontaneous and evoked neurotransmitter release, highlighting the importance of the C-terminus in regulating the effect of Cpx on these two modes of synaptic vesicle fusion.

Experimental methods

Drosophila genetics and molecular cloning

Drosophila melanogaster were cultured on standard medium at 25 °C. Genomic evaluation of *Drosophila cpx* regions made use of Flybase (Tweedie et al., 2009). DmCpx7A was cloned from a *Drosophila* cDNA clone obtained from the *Drosophila* Genomics Research Center (clone ID GH27718). DmCpx7B was cloned from a first-strand cDNA synthesized using the High Capacity cDNA Reverse Transcription Kit (Applied Biosystems) from total RNA purified from Canton S adults using the RNeasy Mini Kit (Qiagen). PCR products were subcloned into the pValum vector downstream of a 10xUAS cassette. UAS-DmCpx7A, UAS-DmCpx7B, UAS-GFP-DmCpx7A, UAS-mCherry-DmCpx7A, UAS-GFP-DmCpx7B and UAS-mCherry-DmCpx7B were injected by Genetic Services Inc. (Cambridge, MA) into y^1v^1;;P{CaryP} attP2 embryos for a third chromosome insertion as described (Ni et al., 2008). UAS lines were then recombined into the cpx^{SH1} null mutant background (Huntwork and Littleton, 2007). The $elav^{C155}$-Gal4 driver was used for pan-neuronal expression of transgenes. The cpx^{572} mutant was generated by feeding EMS to Canton S males and testing non-complementation of 5000 mutagenized lines with cpx^{SH1}.

Immunostaining and western blot analysis

Immunostaining was performed on wandering 3rd instar larvae after rearing at 25 °C as described previously (Huntwork and Littleton, 2007; Rieckhof et al., 2003). Anti-DmCpx antiserum (1:500) (Huntwork and Littleton, 2007) with a secondary antibody conjugated to Alexa-488 (Molecular Probes, Carlsbad, CA) and goat anti-HRP antiserum conjugated to DyLight 549 (Jackson ImmunoResearch) (1:1000, Jackson ImmunoResearch, West Grove, PA) were used for immunostaining. Immunoreactive proteins were visualized on a Zeiss Pascal Confocal microscope system with PASCAL software (Carl Zeiss MicroImaging, Inc.).

Western blotting of whole adult head lysates was performed using standard laboratory procedures with anti-DmCpx (1:5000). For quantitative western analysis, adult heads were collected and lysed in 10 μl of 4× Laemmli sample buffer/head (8% SDS, 40% glycerol, 20% 2-mercaptoethanol, 0.02% bromophenol blue, 250 mM Tris HCl, pH 6.8). The equivalent of one head was loaded per lane. Equal loading was assayed using anti-arginine kinase at 1:5000. Western blots were imaged using an Odyssey infrared scanner (Li-Cor). The intensity of each DmCpx band was standardized to the intensity of the corresponding arginine kinase band using Odyssey software (Li-Cor). Samples were prepared and loaded in triplicate for a total of nine measurements.

FRAP analysis

Larvae expressing DmCpx7A-GFP or DmCpx7B-GFP were preselected for FRAP experiments based on GFP intensity. 3rd instar larvae were dissected in HL3 solution and pinned on silgard plates. Nerves were cut to eliminate muscle contractions. NMJs were imaged under 40× magnification using a Perkin Elmer spinning disk confocal microscope equipped with a Hamamatsu C9100-13 camera. Areas of the bouton were bleached using a 50 mW 488 laser operating on maximum power. Confocal images were collected before and after bleaching and fluorescence recovery was followed for 1 min with 10 s intervals. Total fluorescence of the bleached areas was measured before and after bleaching. Fluorescence recovery was measured as delta F between bleached areas and the recovering time point and plotted as a percentage of the initial fluorescence.

In situ hybridization

Sense and antisense RNA probes labeled with digoxigenin (Roche) were generated by in vitro transcription of the first 500 bp in the 3′ untranslated regions of both Cpx7A and Cpx7B. In situ hybridization was carried out as described previously (Tautz and Pfeifle, 1989).

Quantitative RT-PCR

For absolute quantification of DmCpx7A and DmCpx7B levels, total RNA was extracted from ten adult Canton S flies or 3rd instar larvae using an RNeasy Mini Kit (Qiagen) and treated with DNase I (Ambion) according to the manufacturers' instructions. DNase I was then removed from each sample with the RNeasy Mini Kit. Single stranded cDNA was synthesized in a total volume of 20 μL from 1 μg of total RNA using the High Capacity cDNA Reverse Transcription Kit (Applied Biosystems) according to the manufacturer's protocol. PCR was carried out in quadruplicate for each of three independent total RNA samples per genotype in optical 96-well plates (Applied Biosystems) for a total of 12 measurements per data point. The reaction mixtures were as follows: 25 μL of 2× QuantiTect SYBR Green PCR Master Mix (Qiagen), 300 nM forward primer, 300 nM reverse primer, and 5 μL of single stranded cDNA (see above) in a total volume of 50 μL. The thermal cycling conditions were 15 min at 95 °C, followed by 40 cycles of 15 s at 94 °C, 30 s at 54 °C, and 30 s at 72 °C. A final dissociation step was carried out to evaluate product integrity, and reaction samples were run on a 1.2% agarose gel and stained with ethidium bromide. The absolute levels of DmCpx7A and DmCpx7B were calculated using SDS software (Applied Biosystems) by comparison to a standard curve of DmCpx7A and DmCpx7B mRNA, respectively, transcribed in vitro. Values were normalized to the level of DmCpx7A transcripts in adult flies. For relative quantification of mRNA levels in the activity-dependence experiments (Fig. 2D), the levels of DmCpx7A and DmCpx7B were calculated using SDS software (Applied Biosystems) by the $2^{-\Delta\Delta Ct}$ method using actin (Act88F) as an internal control and untreated wild-type (Canton S) animals as a calibrator. Samples were prepared in triplicate. The primer sequences were as follows: Act88F forward 5′-ACTTCTGCTGGAAGGTGGAC-3′ and reverse 5′-ATCCGCAAGGATCTGTATGC-3′, DmCpx7A forward 5′-CCCCCAAGAAGAGCCCAATC-3′ and reverse 5′-CACTGCATGACACA TTTTCCCTCTAT-3′, and DmCpx7B forward 5′-CGCCGAAGCGGAGCA GGAAGAG-3′ and reverse 5′-GGGCGTGCTGGTGTGGGTGTCT-3′.

Electrophysiological analysis

Postsynaptic currents from the specified genotypes were recorded at segment A3 of the ventral longitudinal muscle 6 in 3rd instar larvae using two-electrode voltage clamp with a −80 mV holding potential in modified HL3 solution (in mM: 10 $NaHCO_3$, 5 KCl, 4 MgCl, 5 HEPES, 70 NaCl, 5 trehalose, 115 sucrose, pH 7.2). Final Ca^{2+} concentration was adjusted to the desired level indicated in the text. Data acquisition was performed using Axoscope 9.0 software. Quantal content was estimated by dividing the current integral of nerve-evoked currents by the current integral from individual quanta. Motor nerves innervating the musculature were severed and placed into a suction electrode so action potential stimulation could be applied at the indicated frequencies using a programmable stimulator. Electrophysiology analysis was performed using Clampfit 9.0 software (Axon Instruments, Foster City). Statistical analysis and graphs were performed using Origin

Software (OriginLab Corporation, Northampton, MA, USA). Statistical significance was determined using a two-tailed Student's t test. For all data, error bars represent SEM.

Acknowledgments

We thank Krys Foster and Amanda Hartman for help with EMS screening and Robin Stevens for supplying the Synaptogyrin-GFP transgenic line. RAJ was supported by the PEW Latin American Fellow Program in Biomedical Science. This work was supported by NIH grant NS40296 to J.T.L.

References

An, S.J., Grabner, C.P., Zenisek, D., 2010. Real-time visualization of complexin during single exocytic events. Nat. Neurosci. 13, 577–583.
Bracher, A., Kadlec, J., Betz, H., Weissenhorn, W., 2002. X-ray structure of a neuronal complexin–SNARE complex from squid. J. Biol. Chem. 277, 26517–26523.
Brand, A.H., Perrimon, N., 1993. Targeted gene expression as a means of altering cell fates and generating dominant phenotypes. Development 118, 401–415.
Cai, H., Reim, K., Varoqueaux, F., Tapechum, S., Hill, K., Sorensen, J.B., Brose, N., Chow, R.H., 2008. Complexin II plays a positive role in Ca^{2+}-triggered exocytosis by facilitating vesicle priming. Proc. Natl. Acad. Sci. U. S. A. 105, 19538–19543.
Chen, X., Tomchick, D.R., Kovrigin, E., A., c, D., Machius, M., Südhof, T.C., Rizo, J., 2002. Three-dimensional structure of the complexin/SNARE complex. Neuron 33, 397–409.
Cho, R.W., Song, Y., Littleton, J.T., 2010. Comparative analysis of *Drosophila* and mammalian complexins as fusion clamps and facilitators of neurotransmitter release. Mol. Cell. Neurosci. 45, 389–397.
Geppert, M., Goda, Y., Hammer, R.E., Li, C., Rosahl, T.W., Stevens, C.F., Südhof, T.C., 1994. Synaptotagmin I: a major Ca^{2+} sensor for transmitter release at a central synapse. Cell 79, 717–727.
Giraudo, C.G., Eng, W.S., Melia, T.J., Rothman, J.E., 2006. A clamping mechanism involved in SNARE-dependent exocytosis. Science 313, 676–680.
Giraudo, C.G., Garcia-Diaz, A., Eng, W.S., Yamamoto, A., Melia, T.J., Rothman, J.E., 2008. Distinct domains of complexins bind SNARE complexes and clamp fusion in vitro. J. Biol. Chem. 283, 21211–21219.
Giraudo, C.G., Garcia-Diaz, A., Eng, W.S., Chen, Y., Hendrickson, W.A., Melia, T.J., Rothman, J.E., 2009. Alternative zippering as an on–off switch for SNARE-mediated fusion. Science 323, 512–516.
Guan, Z., Saraswati, S., Adolfsen, B., Littleton, J.T., 2005. Genome-wide transcriptional changes associated with enhanced activity in the *Drosophila* nervous system. Neuron 48, 91–107.
Higuchi, M., Single, F.N., Köhler, M., Sommer, B., Sprengel, R., Seeburg, P.H., 1993. RNA editing of AMPA receptor subunit GluR-B: a base-paired intron–exon structure determines position and efficiency. Cell 75, 1361–1370.
Hobson, R.J., Liu, Q., Watanabe, S., Jorgensen, E.M., 2011. Complexin maintains vesicles in the primed state in *C. elegans*. Curr. Biol. 21, 106–113.
Hoopengardner, B., Bhalla, T., Staber, C., Reenan, R., 2003. Nervous system targets of RNA editing identified by comparative genomics. Science 301, 832–836.
Huntwork, S., Littleton, J.T., 2007. A complexin fusion clamp regulates spontaneous neurotransmitter release and synaptic growth. Nat. Neurosci. 10, 1235–1237.
Kaeser-Woo, Y.J., Yang, X., Sudhof, T.C., 2012. C-terminal complexin sequence is selectively required for clamping and priming but not for Ca^{2+} triggering of synaptic exocytosis. J. Neurosci. 32, 2877–2885.
Karatekin, E., Giovanni, J.D., Iborra, C., Coleman, J., O'Shaughnessy, B., Seagar, M., Rothman, J.E., 2010. A fast, single-vesicle fusion assay mimics physiological SNARE requirements. Proc. Natl. Acad. Sci. U. S. A. 107, 3517–3521.
Littleton, J.T., Bellen, H.J., Perin, M.S., 1993. Expression of synaptotagmin in *Drosophila* reveals transport and localization of synaptic vesicles to the synapse. Development 118, 1077–1088.
Malsam, J., Seiler, F., Schollmeier, Y., Rusu, P., Krause, J., Söllner, T., 2009. The carboxy-terminal domain of complexin I stimulates liposome fusion. Proc. Natl. Acad. Sci. U. S. A. 106, 2001–2006.
Martin, J.A., Hu, Z., Fenz, K.M., Fernandez, J., Dittman, J.S., 2011. Complexin has opposite effects on two modes of synaptic vesicle fusion. Curr. Biol. 21, 97–105.
Maximov, A., Tang, J., Yang, X., Pang, Z.P., Südhof, T.C., 2009. Complexin controls the force transfer from SNARE complexes to membranes in fusion. Science 323, 516–521.
McMahon, H.T., Missler, M., Li, C., Südhof, T.C., 1995. Complexins: cytosolic proteins that regulate SNAP receptor function. Cell 83, 111–119.
Mohrmann, R., de Wit, H., Verhage, M., Neher, E., Sorensen, J.B., 2010. Fast vesicle fusion in living cells requires at least three SNARE complexes. Science 330, 502–505.
Ni, J.Q., Markstein, M., Binari, R., Pfeiffer, B., Liu, L.P., Villalta, C., Booker, M., Perkins, L., Perrimon, N., 2008. Vector and parameters for targeted transgenic RNA interference in Drosophila melanogaster. Nat. Methods 5, 49–51.
Pabst, S., Hazzard, J.W., Antonin, W., Südhof, T.C., Jahn, R., Rizo, J., Fasshauer, D., 2000. Selective interaction of complexin with the neuronal SNARE complex. Determination of the binding regions. J. Biol. Chem. 275, 19808–19818.
Pickering, B.M., Willis, A.E., 2005. The implications of structured 5′ untranslated regions on translation and disease. Semin. Cell Dev. Biol. 16, 39–47.
Reim, K., Mansour, M., Varoqueaux, F., McMahon, H.T., Südhof, T.C., Brose, N., Rosenmund, C., 2001. Complexins regulate a late step in Ca^{2+}-dependent neurotransmitter release. Cell 104, 71–81.
Reim, K., Wegmeyer, H., Brandstätter, J.H., Xue, M., Rosenmund, C., Dresbach, T., Hofmann, K., Brose, N., 2005. Structurally and functionally unique complexins at retinal ribbon synapses. J. Cell Biol. 169, 669–680.
Rieckhof, G.E., Yoshihara, M., Guan, Z., Littleton, J.T., 2003. Presynaptic N-type calcium channels regulate synaptic growth. J. Biol. Chem. 278, 41099–41108.
Schaub, J.R., Lu, X., Doneske, B., Shin, Y.-K., McNew, J.A., 2006. Hemifusion arrest by complexin is relieved by Ca^{2+}-synaptotagmin I. Nat. Struct. Mol. Biol. 13, 748–750.
Seiler, F., Malsam, J., Krause, J.M., Söllner, T.H., 2009. A role of complexin–lipid interactions in membrane fusion. FEBS Lett. 583, 2343–2348.
Strenzke, N., Chanda, S., Kopp-Scheinpflug, C., Khimich, D., Reim, K., Bulankina, A.V., Neef, A., Wolf, F., Brose, N., Xu-Friedman, M.A., et al., 2009. Complexin-I is required for high-fidelity transmission at the endbulb of Held auditory synapse. J. Neurosci. 29, 7991–8004.
Südhof, T.C., Rothman, J.E., 2009. Membrane fusion: grappling with SNARE and SM proteins. Science 323, 474–477.
Tautz, D., Pfeifle, C., 1989. A non-radioactive in situ hybridization method for the localization of specific RNAs in *Drosophila* embryos reveals translational control of the segmentation gene hunchback. Chromosoma 98, 81–85.
Tweedie, S., Ashburner, M., Falls, K., Leyland, P., McQuilton, P., Marygold, S., Millburn, G., Osumi-Sutherland, D., Schroeder, A., Seal, R., Zhang, H., FlyBase Consortium, 2009. Flybase: enhancing *Drosophila* gene ontology annotations. Nucleic Acids Res. 37, D555–D559.
van den Bogaart, J., Holt, M.G., Bunt, G., Riedel, D., Wouters, F.S., Jahn, R., 2010. One SNARE complex is sufficient for membrane fusion. Nat. Struct. Mol. Biol. 17, 358–364.
Xu, J., Mashimo, T., Südhof, T.C., 2007. Synaptotagmin-1, -2, and -9: Ca^{2+} sensors for fast release that specify distinct presynaptic properties in subsets of neurons. Neuron 54, 567–581.
Xue, M., Reim, K., Chen, X., Chao, H.-T., Deng, H., Rizo, J., Brose, N., Rosenmund, C., 2007. Distinct domains of complexin I differentially regulate neurotransmitter release. Nat. Struct. Mol. Biol. 14, 949–958.
Xue, M., Stradomska, A., Chen, H., Brose, N., Zhang, W., Rosenmund, C., Reim, K., 2008. Complexins facilitate neurotransmitter release at excitatory and inhibitory synapses in mammalian central nervous system. Proc. Natl. Acad. Sci. U. S. A. 105, 7875–7880.
Xue, M., Lin, Y.Q., Pan, H., Reim, K., Deng, H., Bellen, H.J., Rosenmund, C., 2009. Tilting the balance between facilitatory and inhibitory functions of mammalian and *Drosophila* Complexins orchestrates synaptic vesicle exocytosis. Neuron 64, 367–380.
Xue, M., Craig, T.K., Xu, J., Chao, H.-T., Rizo, J., Rosenmund, C., 2010. Binding of the complexin N terminus to the SNARE complex potentiates synaptic-vesicle fusogenicity. Nat. Struct. Mol. Biol. 17, 568–575.
Yoshihara, M., Littleton, J.T., 2002. Synaptotagmin I functions as a calcium sensor to synchronize neurotransmitter release. Neuron 36, 897–908.
Zhang, F.L., Casey, P.J., 1996. Protein prenylation: molecular mechanisms and functional consequences. Annu. Rev. Biochem. 65, 241–269.
Zuker, M., 2003. Mfold web server for nucleic acid folding and hybridization prediction. Nucleic Acids Res. 31, 3406–3415.